

# PADC nuclear track detector for ion spectroscopy in laser-plasma acceleration

M. Seimetz<sup>\*1</sup>, J. Peñas<sup>2</sup>, J.J. Llerena<sup>2</sup>, J. Benlliure<sup>2</sup>, J. García López<sup>3,4</sup>, M.A. Millán-Callado<sup>3,4</sup>, J.M. Benlloch<sup>1</sup>

1-Instituto de Instrumentación para Imagen Molecular (I3M), CSIC-Universitat Politècnica de València, Valencia, Spain

2-Instituto Galego de Física das Altas Enerxías (IGFAE), Universidade de Santiago de Compostela, Santiago de Compostela, Spain

3-Departamento de Física Atómica, Molecular y Nuclear, Universidad de Sevilla, Sevilla, Spain

4-Centro Nacional de Aceleradores (CNA), Universidad de Sevilla-CSIC-Junta de Andalucía, Sevilla, Spain

\*Corresponding author. Contact: mseimetz@i3m.upv.es



## 1. Background and objectives

The transparent polymer PADC (CR-39) is widely used for ion detection in laser-plasma interactions. PADC combines a high sensitivity and high specificity with inertness towards electromagnetic noise. We have developed techniques for the identification of different ion species and for the determination of particle energies based on the track characteristics. Calibration samples irradiated with mono-energetic proton and carbon ion beams allow for systematic studies of the corresponding track diameters. In addition, hardware and software tools have been developed for the automatic scanning and track analysis. We have observed significant differences in the response of two types of PADC plastics. Our results will be applied to laser-plasma acceleration of protons and carbon ions. They may be useful for other fields as well such as the dosimetry of target fragments in ion therapy [1].

## 2. Calibration with mono-energetic proton and ion beams

### Data taking

More than 300 PADC plates of different types and production series (25 samples per vacuum cycle) have been irradiated at the 3 MV tandem accelerator of CNA. Particle energies: 0.2-3 MeV (protons), 0.6-12 MeV (C ions).

Carbon ions of different charge states produce a coherent distribution of track diameters as remaining electrons are stripped off at the PADC surface.



Control elements for the beam position (phosphor screen), spot size (RCF), and particle flux (online monitor) with pulsed beam have been installed on the target holder inside the vacuum chamber (Fig. 1).

Figure 1: Holder for 25 PADC plates and beam control elements.

### Etching and image acquisition

With the aim of reducing the etching time after use in laser acceleration experiments we have chosen a high etch bath temperature (6.25N NaOH, 90°C, 4 hours).

Three microscopes have been tested to scan the PADC plates (Fig. 2):

- Radosys NanoReader: 6 images/plate, 3 µm pixel size (standard for Ra-alpha tracks; resolution insufficient for protons).
- Lab microscope with 2D motor control: entire chip area, 1.2 µm pixel size.
- Radosys PT10: 140 images/plate (40% of total surface), 0.3 µm pixel size; no focus control during scan.

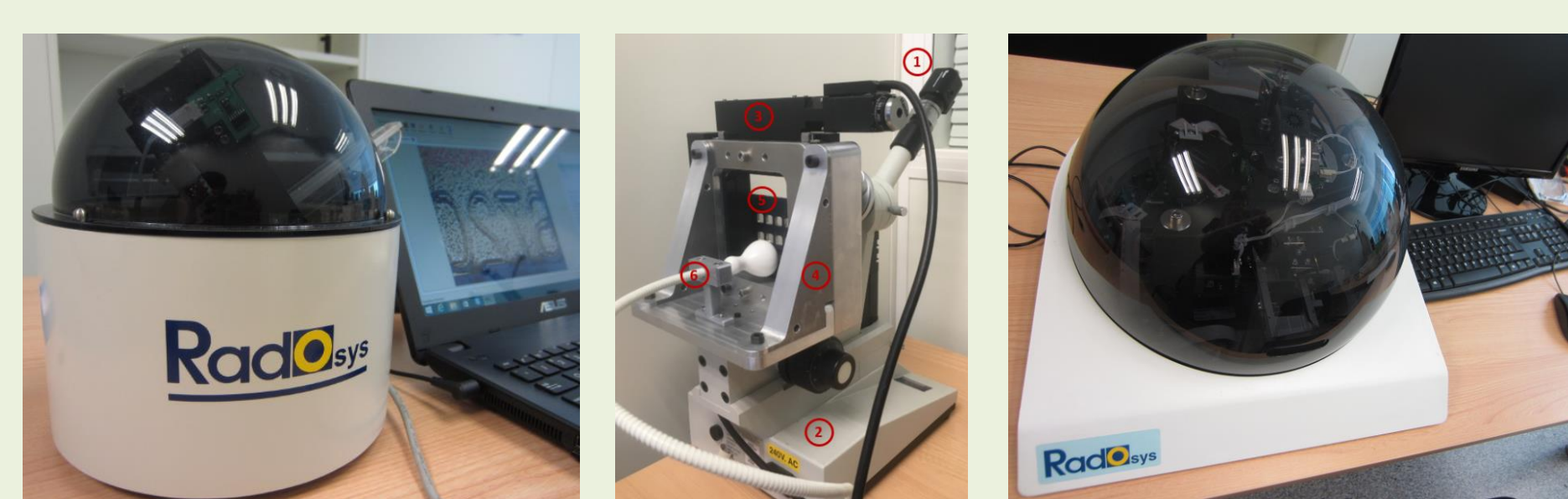


Figure 2: Track readers: NanoReader, lab microscope, PT10.

### Image selection and analysis

An analysis procedure applicable to calibration samples (uniform track diameters) as well as laser-ion samples has been developed.

Step 1: Elimination of images with overlapping tracks, surface impurities, or diffuse track borders; up to 90% of each set of photographs are rejected. Manual selection or automatic recognition based on machine learning.

Step 2: Identification of circular patterns and measurement of track diameters. Basic method: Hough transform combined with edge detection algorithms.

Our calibration samples contain major numbers of circular tracks with very similar diameters for each ion energy. The absolute track diameters depend strongly on the type of PADC (Fig. 3).

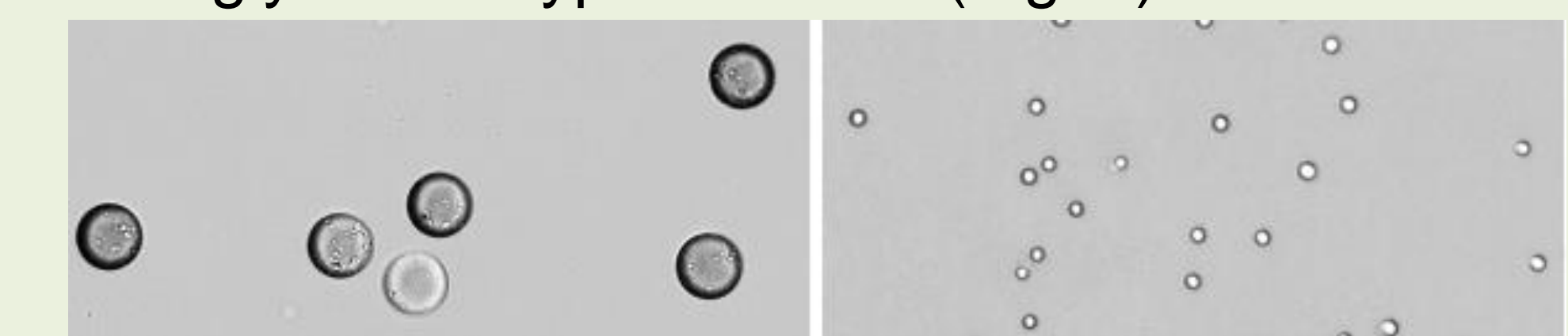


Figure 3: 1 MeV proton tracks on "S" and "RS39" type SSDs.

## 3. Results

### PADC, "S" type, protons

Radosys S series SSDs have been applied in our previous work [2]. Calibration data from 2015 showed a characteristic maximum for the track diameters as a function of proton energy. This is in qualitative agreement with previous findings using SSDs from different providers (Pershore [3], TASL [4, 5], Fukuvi [6]). Here, we have repeated the calibration with a control sample (Fig. 4).

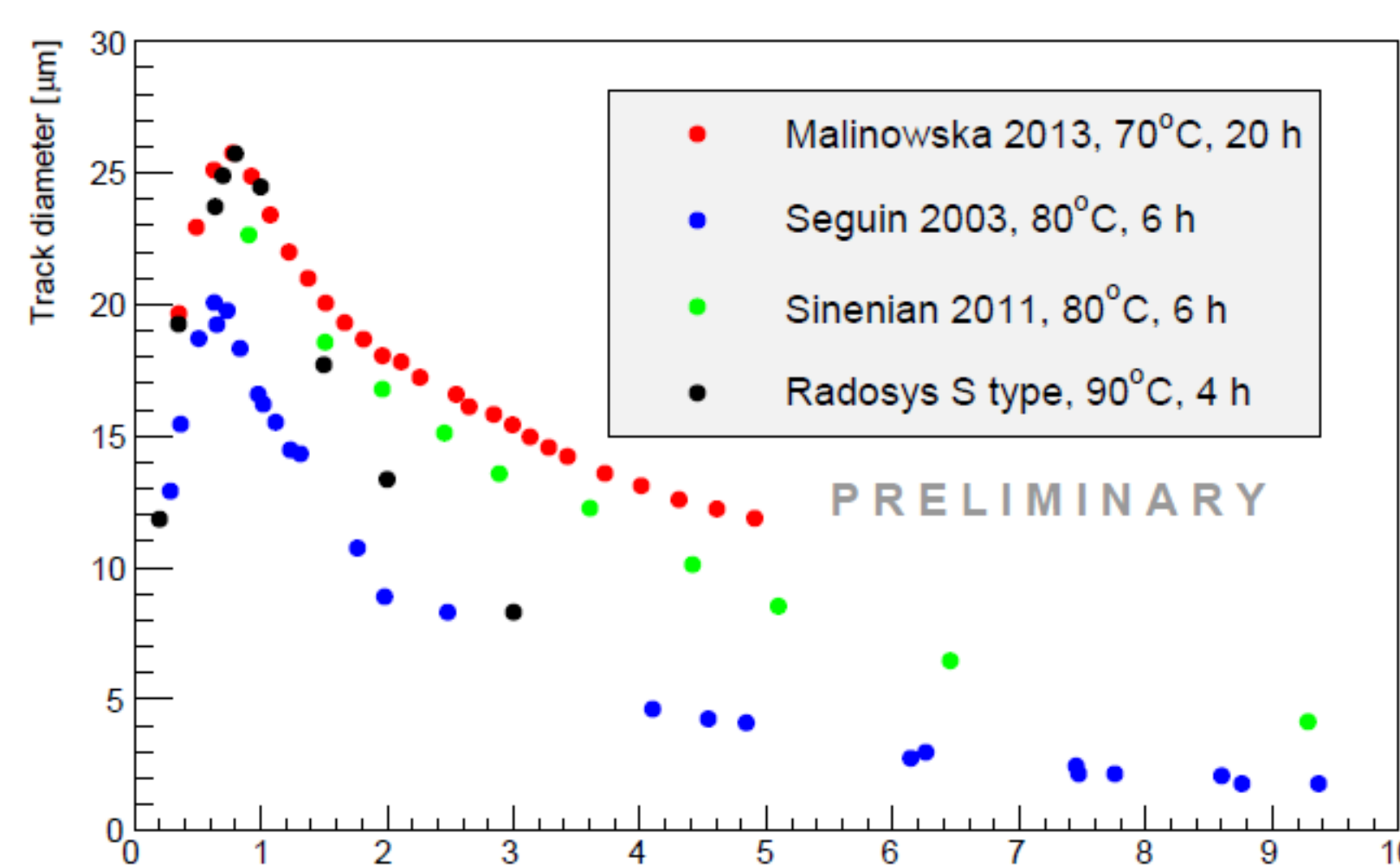


Figure 4: Track diameters of protons on S type (equiv.) SSDs.

### PADC, "RS39" type, protons

We have realised the first calibration of Radosys RS39 SSDs with protons. The response of this material is qualitatively very different: It does not show any sensitivity to protons above 1.2 MeV, and a plateau region in the track diameters is observed instead of a narrow maximum (Fig. 5). A similar comparison of two types of PADC (CR-39 and PM-355, brand names of Pershore) has been reported in [7].

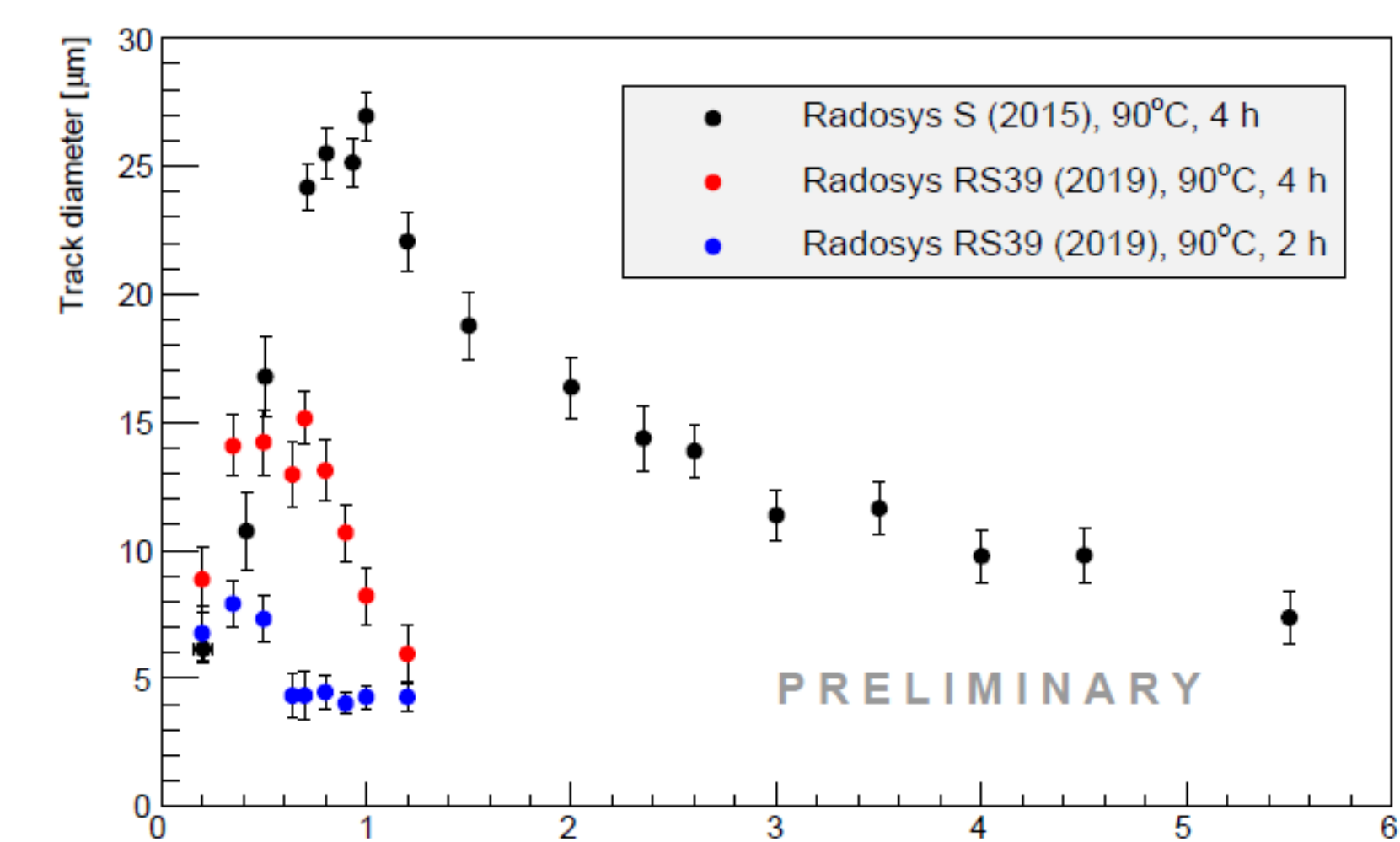


Figure 5: Track diameters of protons on Radosys S and RS39.

### PADC, carbon ions

Calibration measurements of the response of PADC to carbon ions are still rare and show significant, quantitative deviations [8,9]. At the lower end of the spectrum, track diameters increase with higher ion energies. Our data confirm this trend for both types of PADC employed (Fig. 6). Towards higher energies a plateau regime may be present [10].

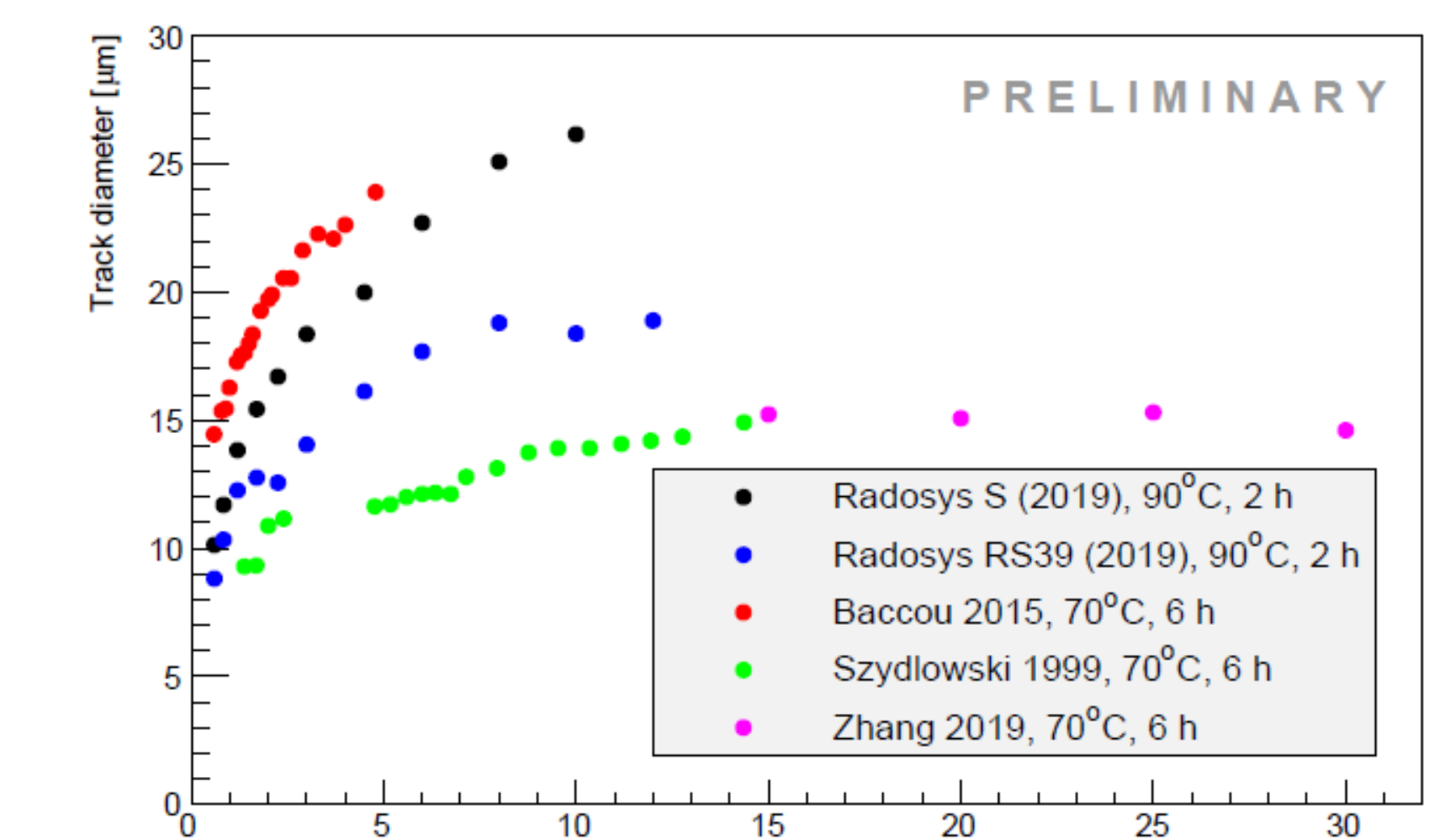


Figure 6: Track diameters of carbon ions.

## 4. Application to proton and ion spectroscopy

The S type SSDs show a unique relation between proton energies and track diameters below the maximum (0-1 MeV, Fig. 7). This allows for obtaining  $E_p$  as long as it can be ruled out that protons with energies higher than 1 MeV hit the PADC surface. To this purpose, thin absorbers are placed in front of the PADC plates (Fig. 7). This method has been applied for laser-accelerated protons from a 3 TW/55 fs Ti:Sapphire laser (Fig. 8) [2,11]. RS39 type SSDs may be used to detect protons of 0.2-1.2 MeV, albeit with reduced precision. Further, RS39 may be useful to discriminate between protons and carbon ions thanks to their different track diameters under the same etching conditions. This will be tested at the 50 TW/25 fs laser of L2A2 (Santiago de Compostela).

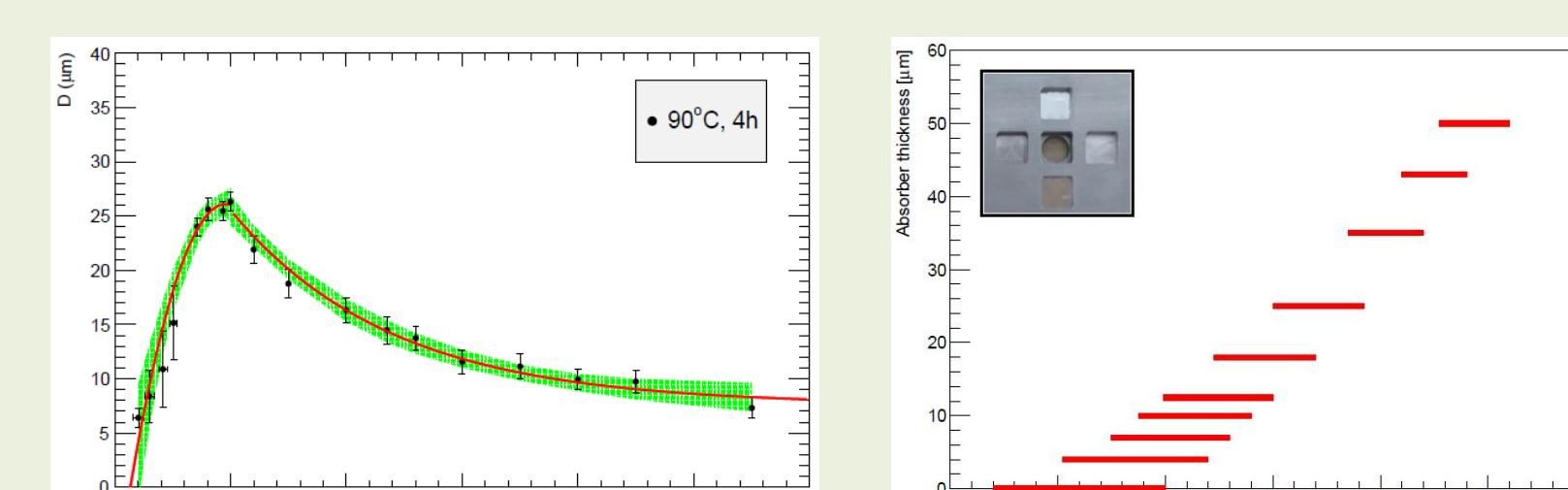


Figure 7: Proton calibration [2]; intervals for different absorbers.

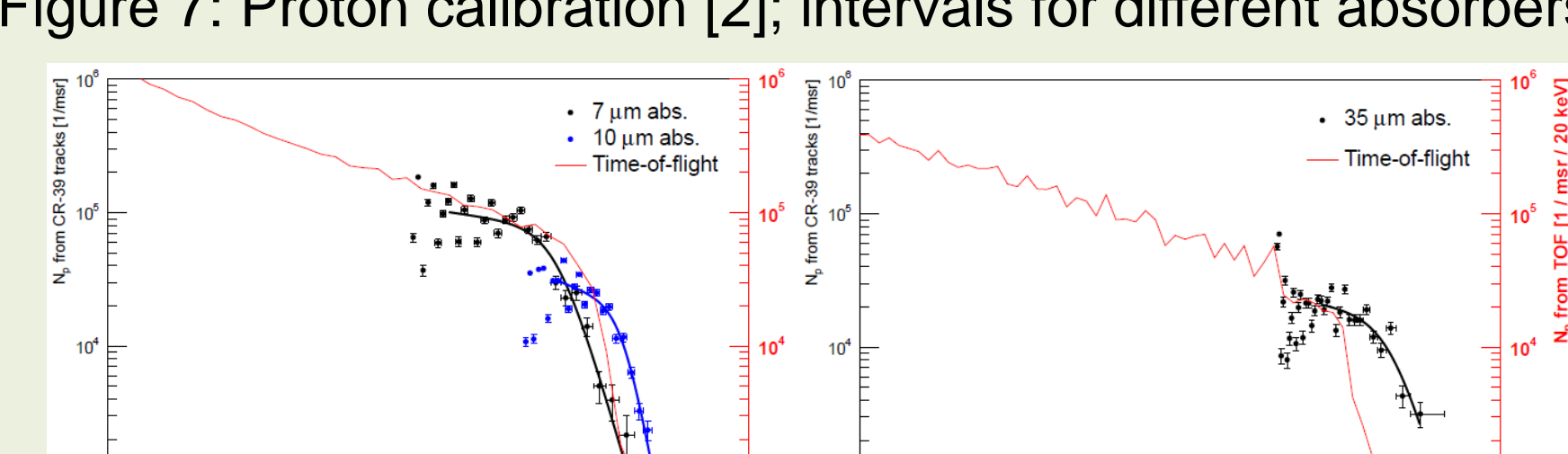


Figure 8: Proton spectra obtained with S type PADC [2].

## References

- [1] S. Kodaira *et al.*, Sci. Rep. **9**, 3708 (2019)
- [2] M. Seimetz *et al.*, RSI **89**, 023302 (2018)
- [3] A. Malinowska *et al.*, RSI **84**, 073511 (2013)
- [4] F.H. Séguin *et al.*, RSI **74**, 975 (2003)
- [5] N. Sinenian *et al.*, RSI **82**, 103303 (2011)
- [6] D. Xiaojiao *et al.*, NIM A **609**, 190 (2009)
- [7] M. Sadowski *et al.*, R. Meas. **25**, 175 (1995)
- [8] C. Baccou *et al.*, RSI **86**, 083307 (2015)
- [9] A. Szydlowski *et al.*, R. Meas. **31**, 259 (1999)
- [10] Y. Zhang *et al.*, Nucl. Sci. Tech. **30**, 87 (2019)
- [11] P. Bellido *et al.*, JInst **12**, T05001 (2017)

## Acknowledgements

Project funded by CSIC, grant no. 2018501082. This work has been developed in close collaboration with Radosys Ltd. (Budapest) which provided nuclear track detector material and readout equipment. The authors acknowledge the contributions and commitment of the CNA accelerator operators.

